

MALAYSIAN JOURNAL OF ANALYTICAL SCIENCES

Journal homepage: https://mjas.analis.com.my/



Research Article

Design and evaluation of a benzimidazole-based nickel(II) catalyst for the Suzuki reaction

Norul Azilah Abdul Rahman, Noor Azmira Rahim, Najwa Asilah M Shamsuddin, and Nur Rahimah Said*

School of Chemistry and Environment, Faculty of Applied Sciences Universiti Teknologi MARA (UiTM), Cawangan Negeri Sembilan, Kampus Kuala Pilah, 72000 Kuala Pilah, Negeri Sembilan, Malaysia

*Corresponding author: nurra1435@uitm.edu.my

Received: 9 July 2025; Revised: 17 September 2025; Accepted: 23 September 2025; Published: 16 October 2025

Abstract

Nickel catalysts offer significant advantages over palladium-based systems, being more cost-effective and environmentally sustainable for the Suzuki reaction. This study reported on the design and synthesis of a new benzimidazole-based nickel(II) catalyst, [Bis(1,3-bis(4-chlorobenzyl)benzimidazole)]dibromonickel(II) complex (Ni-CAT). The catalyst was synthesised in two steps: firstly, the ligand was prepared via the reaction of benzimidazole with 4-chlorobenzyl bromide, and secondly by coordination with nickel(II). Both the ligand and Ni-CAT were comprehensively characterised by using FAAS, FTIR, NMR (¹H and ¹³C), UV-Vis spectroscopy, and XRD. Results confirmed the successful synthesis of the target complex. A preliminary complexation study revealed that a 1:2 metal-to-ligand ratio, was consistent with the proposed structure of Ni-CAT. Catalytic performance of Ni-CAT was evaluated in the Suzuki carbon–carbon coupling of aryl bromides with phenylboronic acid. Effects of different aryl bromides, solvents and bases were systematically studied, with catalytic activity monitored by GC-FID. High conversion rate of 91.7% was achieved under optimised conditions of 1-bromo-4-nitrobenzene, 0.25 mmol% Ni-CAT catalyst loading, methanol as solvent, and K₂CO₃ as base at 65 °C for 2 h. This study established a novel benzimidazole-derived nickel(II) complex as an efficient and sustainable alternative to palladium catalysts in the Suzuki reaction, demonstrating excellent activity under mild conditions with exceptionally low catalyst loading.

Keywords: benzimidazole ligand, carbon-carbon coupling reaction, nickel(II) benzimidazole catalyst, carbene carbon, Suzuki reaction

Introduction

Suzuki reaction involves reactions between aryl or vinyl boronic acid and aryl or vinyl halides in the presence of metal catalyst [1, 2]. Most studies had focused on the Suzuki reaction due to usage of organoboron compounds, which serve as reagents which provide high selectivity and stability in cross-coupling reactions. Several intermediates in the pharmaceutical, agriculture and natural products industries are synthesised by using this method. Suzuki reaction offer numerous benefits, such as ready availability of reactants, low toxicity and stability towards air and water [3].

Recent developments in the Suzuki reaction had focused on enhancing its efficiency and environmental sustainability. Researchers had explored new catalysts for the Suzuki reaction, moving beyond traditional palladium (Pd) to other

metals, such as nickel (Ni) [4, 5]. Nickel catalysts had gained significant attention over the past years due to their unique performance in the Suzuki reaction. Initially, nickel was thought to be highly reactive and less selective because it is able to access different oxidation states. Additionally, nickel catalysts can activate less reactive electrophiles, such as aryl chlorides, unactivated alkyl electrophiles, and various C-O bonds. Studies showed that nickel catalysts exhibited high efficiency catalytic the Suzuki reactions [1,6-8]. Furthermore, nickel offers several advantages over other metal catalysts, being cheaper, more sustainable, and environmentally friendly [6, 9].

Structure of the donor ligand also plays a crucial role in determining the catalytic efficiency of nickel catalysts. Ligand structure affects the stability of active species and lifetime of catalyst [10, 11].

Benzimidazole was found to be efficient and productive for heterocycles in chemistry [12, 13]. Benzimidazole as a nitrogen-based ligand is a suitable ligand in catalyst structure due to its strong sigma-donor and weak pi-acceptor abilities, low toxicity, inexpensive and stability [14]. Studies showed that compounds containing benzimidazole and its complexes had a variety of applications in biological research, including anticancer, antifungal, and antidiabetic agents [13]. Benzimidazole is also used as an ionophore in sensors and as a ligand for palladium catalysis [15-20].

To date, there are limited studies explored the catalytic potential of [Bis(1,3-bis(4-chlorobenzyl) benzimidazole)] dibromonickel(II) (Ni-CAT) complex in the Suzuki reaction. Therefore, evaluating this complex as a new benzimidazole-based nickel(II) catalyst is necessary to address cost-effectiveness, and efficiency in the Suzuki reaction.

Materials and Methods Chemicals and instruments

chemicals and solvents obtained from commercial suppliers were used without further purification. The chemicals and solvents used in this study included nickel(II) chloride (NiCl₂, Merck), benzimidazole (Merck), 4-chlorobenzyl bromide (Merck), methanol (MeOH, Merck), 1,4-dioxane (Fisher), dimethyl sulfoxide (DMSO, Merck), potassium carbonate (K2CO3, Merck), sodium carbonate (Na₂CO₃, Sigma-Aldrich), sodium acetate (NaOAc, Merck), triethylamine (Et₃N, Merck), sodium hydroxide (NaOH, Sigma), N,Ndimethylacetamide (DMA, R&M Chemicals), phenylboronic acid (Sigma-Aldrich), 1-bromo-4nitrobenzene (Merck), 1-bromobenzene (Merck), 4bromoacetophenone 4-bromoanisole (Merck). (Merck), and nitrogen gas.

All synthesis products were collected by vacuum filtration and oven dried. The confirmation of each product was carried out by using Flame Atomic Absorption Spectroscopy (FAAS), Attenuated Total Reflection–Fourier Transform Infrared (ATR-FTIR) spectroscopy, ¹H and ¹³C Nuclear Magnetic Resonance (NMR), UV–Visible spectroscopy (UV–Vis), and powder X-ray Diffraction (PXRD). The catalytic performance of the synthesised complex in the Suzuki reaction was determined by using Gas Chromatography–Flame Ionisation Detection (GC-FID)

Percentage of Ni in the catalyst was measured by using FAAS (Perkin Elmer AAnalyst 400). FTIR spectra were recorded between 4000 cm⁻¹ - 650 cm⁻¹ as attenuated total reflectance (ATR) on a Perkin

Elmer Spectrum 400 FTIR spectrometer. The NMR spectra of the compound were analysed by using ¹H and ¹³C Nuclear Magnetic Resonance (NMR) spectroscopy on a Bruker Advance 400 spectrometer at 400 MHz, with tetramethylsilane (TMS) as the internal standard.

A UV–Vis double-beam spectrophotometer (T80 Series) was used in the range of 200 nm – 500 nm to confirm the formation of complexes by comparing the electronic transitions of ligands and complexes. The diffractogram of the samples was obtained by using PXRD (Empyrean, PANalytical) and recorded over a 2θ range of 2° to 50° with a step size of 0.02° min⁻¹. The X-ray diffractometer was operated at voltage of 40 kV and current of 20 mA.

The catalytic study for the Suzuki reaction performance was analysed by using Agilent 7820A (G4350A) GC with FID and TCD detector, Agilent G4513A Injector by calculating the conversion rate of reactants. The instrument was equipped with HP-5 capillary column (15 m \times 0.25 mm \times 0.25 μm) with Flame Ionisation Detector (GC-FID). The microliter samples were injected at 50 °C (held for 3 min) and final temperature at 250 °C (held for 30 s). Temperature increment was increased at 15 °C/min. The flow rate used was 1.9162 mL/min.

Synthesis of Ni-CAT

The steps of Ni-CAT preparation are shown in **Figure 1**.

Step 1- Preparation of ligand: Benzimidazole (0.295 g, 2.5 mmol) was added into 10 mL of 1,4-dioxane in a three-neck round-bottom flask. The mixture was stirred at room temperature until completely dissolved, followed by the dropwise addition of 4-chlorobenzyl bromide (1.0274 g, 5 mmol). The solution was then refluxed for 24 h. A white precipitate of 1,3-bis[(4-chlorobenzyl)] benzimidazolium bromide ligand appeared at the bottom of flask. The compound was collected by vacuum filtration and washed with 1,4-dioxane (3 × 5 mL) [18].

Step 2- Preparation of complex: In a round-bottom flask, 0.2 mmol of the ligand prepared in Step 1 was stirred with 15 mL of dry methanol until completely dissolved. Then nickel(II) chloride (0.1 mmol) was then added slowly to the ligand solution and the mixture was refluxed for 5 h until the clear solution turned green-blue. After reflux, 37% NaOH (3.5 mL, 2.0 M) was added dropwise over 30 min, producing a cloudy blue solution. The mixture was stirred for a further 24 h at room temperature. The resulting suspension was collected by filtration, washed with

dry methanol, and oven dried for a few minutes. The final product obtained was [Bis(1,3-bis(4-chlorobenzyl)benzimidazole)]dibromonickel(II) complex (Ni-CAT) [18].

Preliminary complexation study

UV–Vis titration experiments were conducted to determine the stoichiometry of complex formation between the synthesised ligand and Ni²⁺. Individual solutions of the ligand (2.5×10^{-5} M) and NiCl₂ (1.0×10^{-4} M) in DMSO were prepared. A 2.5 mL aliquot of the ligand solution was placed in a cuvette and titrated with the Ni²⁺ solution until the metal-to-ligand ratio reached 2:1. UV–Vis spectra were recorded at approximately 5-min intervals between 260 nm – 350 nm after each titration [10,18].

Catalytic activity study

The catalytic activity of the synthesised Ni-CAT was evaluated in the Suzuki reaction. 1-bromo-4-nitrobenzene (0.202 g, 1 mmol), phenylboronic acid (0.182 g, 1.5 mmol), potassium carbonate (K₂CO₃, 0.276 g, 2 mmol), Ni-CAT (0.25 mmol%), and 5 mL of MeOH were mixed in a three-neck round-bottom flask. The reaction mixture was refluxed for 2 h in the presence of nitrogen gas at 65 °C (b.p. of MeOH). The catalytic performance was analysed by

GC-FID by using a small amount of the crude product [18, 21].

The steps were repeated with different aryl bromides: 1-bromobenzene (0.157 g, 1 mmol), 4-bromoanisole (0.187 g, 1 mmol), and 4-bromoacetophenone (0.199 g, 1 mmol). The catalytic reaction between aryl bromide and phenylboronic acid in the presence of Ni-CAT is illustrated in **Figure 2**, where R represents -NO₂, -H, -OCH₃, and -COCH₃. The Suzuki reaction was also conducted to study the effect of different solvents (MeOH, DMA, and DMSO) and bases (K₂CO₃, Na₂CO₃, NaOAc, and Et₃N) with 1-bromo-4-nitrobenzene.

Results and Discussion Characterization of Ni-CAT

Characteristics of the ligand and Ni-CAT complex are listed in **Table 1**. Upon complexation, colour of the product changed from white to green-blue powder. Additionally, the melting point increased from 240 °C – 244 °C to above 250 °C, indicating enhanced thermal stability. This change was attributed to the successful coordination of nickel with the ligand. The presence of nickel in the Ni-CAT complex was further supported by FAAS data.

Figure 1. Preparation steps of Ni-CAT

Figure 2. Catalytic reaction of aryl bromide and phenylboronic acid with presence of Ni-CAT

Table 1. Characteristics of synthesis compounds

		Ligand	Ni-CAT
Physical properties	Colour	White, powder	Green-blue, powder
	Melting point, (°C)	240-244	> 250
	Yield, (%)	54.64	69.10
% of Ni metal ion (FAAS data)		-	3.92
Molecular formula		$C_{21}H_{17}N_2Cl_2Br$	$C_{42}H_{32}N_4Cl_4Br_2Ni$
Stoichiometry [Ni ²⁺ : Ligand]		-	1:2

Fourier Transform Infrared (FTIR)

Presence of significant functional groups in both the ligand and Ni-CAT was confirmed by using FTIR spectroscopy (**Table 2**). The FTIR spectra of ligand and Ni-CAT complex were recorded over a scan range of 4000 cm⁻¹– 650 cm⁻¹, as shown in **Figure 3**. In the ligand spectrum, C=N stretching band was observed at 1561.53 cm⁻¹. This lower frequency was attributed to π -electron delocalisation within the benzimidazolium ring, which reduced the typical (unconjugated) C=N stretching frequency [18, 22]. The observed functional groups of synthesis ligand were consistent with those reported in previous studies [18, 23].

Upon coordination with nickel, the C=N stretching band disappeared, indicating the formation of a metal-ligand complex. A new sharp band corresponding to the C-N bond appeared at 1663 cm⁻¹, replacing the original C=N band. Notably, this C-N absorption band appeared at an unusually higher frequency, which may be attributed to the electronegativity of nickel. The presence of a polarised Ni-Br bond enhanced the strength of both Ni-C and N-Ccarbene bonds, thereby shifting the absorption to a higher wavenumber [18, 23]. Similar observations were documented whereby metal coordination had led to frequency shifts in FTIR spectra due to enhanced bond polarisation. For instance, Said et al. [18] noted a significant frequency shift following metal coordination, underscoring the concept that ligand-to-metal interactions significantly influence vibrational properties.

Nuclear Magnetic Resonance (NMR)

The number of protons and carbon atoms in the ligand was confirmed by using ¹HNMR and ¹³CNMR spectroscopy, as shown in the spectra **Figure 4** and **Figure 5**. In the ¹HNMR spectrum, a singlet peak

appeared at an upfield chemical shift of 5.84 ppm, corresponding to the methylene protons (-CH2). This shift indicated that the protons were more shielded and absorbed radiation at a higher frequency. In contrast, a multiplet peak for aromatic protons (-CH-Ar) were observed at a slightly downfield chemical shift between 7.48 ppm and 7.99 ppm. This deshielding was attributed to the presence of electron-withdrawing groups such as Cl and N, which decreased the electron density on the aromatic ring through inductive effects. A sharp singlet at 10.18 ppm was assigned to the acidic -CH_{carbene} proton of the benzimidazolium ring. This downfield shift was due to the electron-withdrawing effect of benzyl group attached to the ligand [18, 22]. The significant ¹HNMR chemical shift of ligand is tabulated in Table 3.

In the ¹³CNMR spectrum, a single peak at 143.35 ppm in the downfield region was assigned to the carbene carbon (-CH_{carbene}). Aromatic carbons (-CH-Ar) appeared in the chemical shift range of 127.33 ppm – 133.98 ppm, with variations depending on the neighbouring atoms. A peak at 114.51 ppm, also in the downfield region, was attributed to an aromatic carbon attached to a chlorine atom (-C-Cl) further supporting the presence of an electron-withdrawing substituent. Lastly, a peak at 49.80 ppm, located in the upfield region, corresponded to the methylene (-CH₂) group. Although slightly higher than the typical range of 15 ppm - 40 ppm, this shift was due to the methylene group being bonded to both an aromatic ring and a nitrogen carbene centre [18, 24]. These results strongly supported the successful formation of the benzimidazole ligand and significant ¹³CNMR chemical shift is tabulated in Table 4. However, the ¹HNMR and ¹³CNMR spectra of Ni-CAT complex could not be observed due to the paramagnetic nature of nickel(II) ion [10, 24].

Table 2. Significant functional group of synthesis compounds from FTIR spectra

	Wavelength (cm ⁻¹)		
Functional Group	Ligand	Ni-CAT	
C=N	1561	-	
C-N	1372	1663	
C=C (aromatic)	1494	1521	
C-H (aromatic)	3450	3374	
C-Cl	753	755	

Malays. J. Anal. Sci. Volume 29 Number 5 (2025): 1615

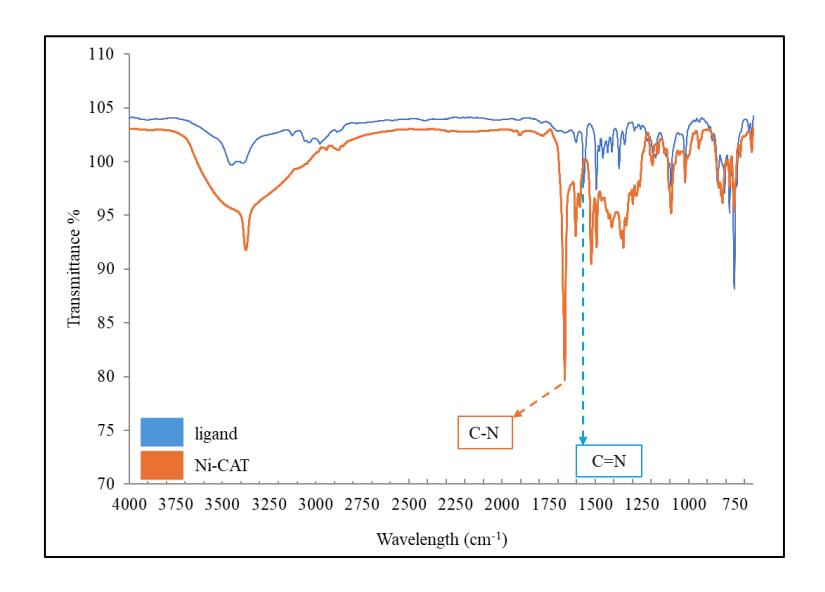


Figure 3. FTIR spectra of synthesis compounds

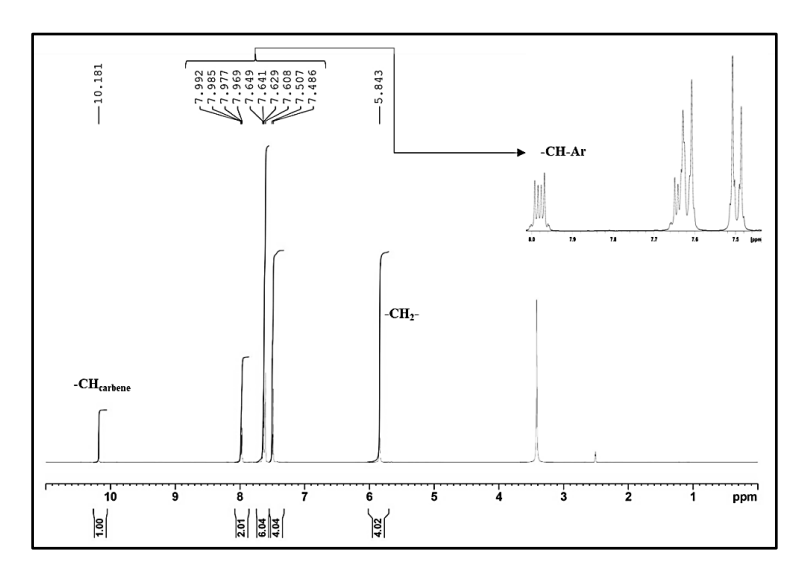


Figure 4. ¹HNMR spectrum of ligand

Table 3. Significant ¹HNMR chemical shift of ligand

Attributions	Chemical Shift, δ (ppm)		
	[multiplicity, number of H]		
-CH _{carbene}	10.18 [s, 1H]		
-CH-Ar	7.99-7.97 [m, 2H]		
-CH-Ar	7.64-761 [m, 6H]		
-CH-Ar	7.51, 7.49 [d, 4H]		
-CH ₂ -	5.84 [s, 1H]		

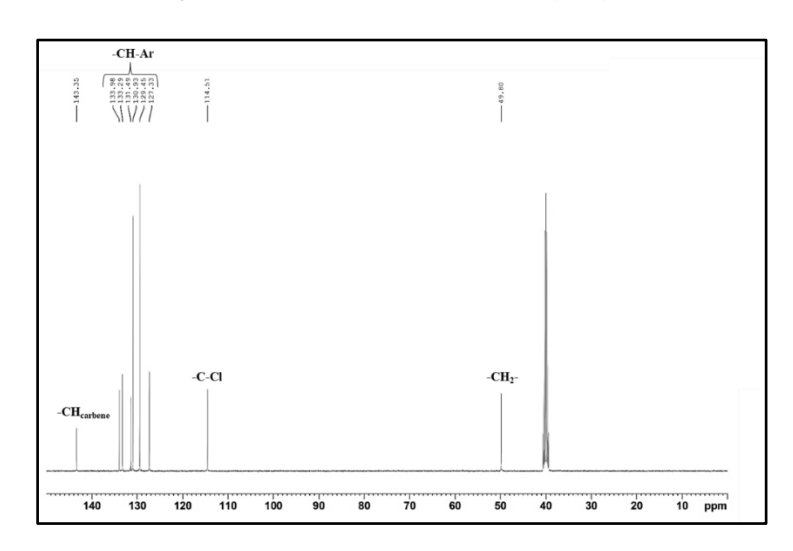


Figure 5. ¹³CNMR spectrum of ligand

Table 4. Significant ¹³CNMR chemical shift of ligand

Attributions	Chemical Shift, δ (ppm)		
-CH _{carbene}	143.35		
-CH-Ar	133.98-127.33		
-C-Cl	114.51		
-CH ₂ -	49.80		

UV-Visible spectroscopy (UV-Vis)

UV-Vis spectroscopy was used to characterise both the ligand and Ni-CAT complex in the range of 240 nm to 500 nm, by using DMSO as the solvent. **Figure 6** shows the absorption spectra of the free ligand and Ni-CAT. Based on spectra, the ligand exhibited two absorption peaks at 271 nm and 300 nm, while Ni-CAT showed peaks at 259 nm and 307 nm. In spectrum of the free ligand, the absorption maximum at 271 nm was attributed to the π - π * transition of the carbene moiety. The weaker and broader absorption band at the lower energy region (300 nm) might be attributed to π - π * ligand-to-ligand charge transfer (LLCT) within the ring, confirming the electronic delocalisation within the benzimidazole framework [25].

When nickel cation was incorporated into the ligand, the UV-Vis spectrum exhibited slightly blue-shifted peaks at 259 nm and red-shifted absorption at 307 nm. The blue-shifted peaks at 259 nm could be correlated with the coordination of N-C_{carbene} bond to nickel ion, which altered the electronic environment surrounding the carbene moiety, as evidenced by studies which found that complexation generally led to a shift in absorption bands due to increased metalligand interactions [26]. Such changes were consistent with observations in literature on nickel complex formation coordinate at C_{carbene} whereby

coordination influenced the π^* orbitals involved in electronic transitions [27, 28].

The second peak observed for the Ni-CAT complex at 307 nm was notable interest as it signified a ligand-to-metal charge transfer (LMCT), suggesting significant electron donation from the ligand to nickel centre. This phenomenon was documented in other transition metal coordinate with C_{carbene} in the ligand, whereby efficient electron transfer occurred due to the favourable overlap between metal dorbitals and ligand p-orbitals, facilitating LMCT transitions [29, 30]. The electromagnetic framework within which the nickel operated played a critical role in these transitions, showcasing how electronic properties of nickel interacted with those of the ligands [31].

Interestingly, while d-d transitions common to transition metals are typically visible above 400 nm, their absence in the Ni-CAT complex could be explained by the paramagnetic nature of complex, as affected by presence of unpaired electrons in the d-orbitals, which precluded the expected electronic transitions from being observed in the UV-Vis spectrum [10, 32]. This observation aligned with findings from previous studies, highlighting that the electronic properties of nickel were significantly modified after complexation, thereby suppressing

typical absorption features associated with electronic transitions within the d-orbital framework [10].

Powder X-ray Diffraction (PXRD)

The powder X-ray diffraction (PXRD) analysis performed on the ligand and resulting Ni-CAT complex provided evidence of successful complex formation and structural alterations coordination. Diffractogram (Figure 7) of the ligand displayed an amorphous nature, showing no characteristic peaks associated with nickel, which is a common feature of uncoordinated ligands in complex formations. This absence of distinct crystalline peaks suggested that the ligand existed in a non-ordered state, which aligned with findings in similar studies whereby amorphous precursor phases important for catalytic applications had been characterised [33, 34].

Upon coordination with nickel, the Ni-CAT complex exhibited a significant diffraction peak at 33.5°, indicating the presence of nickel within a crystalline environment. This peak was attributed to the formation of a crystalline phase in complexes, where metal ions induced structural ordering in the ligands [33, 34]. The increased crystallinity was an important observation, which signified only not complexation of nickel, but also implied a stabilisation effect brought about by coordination, hence enhancing the structural integrity of complex. Such findings supported literature indicating that coordination of metals can enhance crystallinity due to tighter packing and ordered crystal lattices [35].

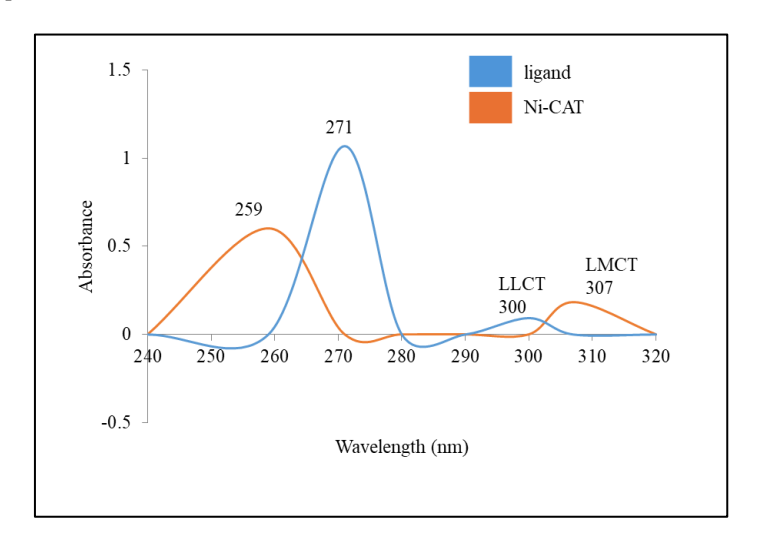


Figure 6. UV-Vis absorption spectra of synthesis compounds

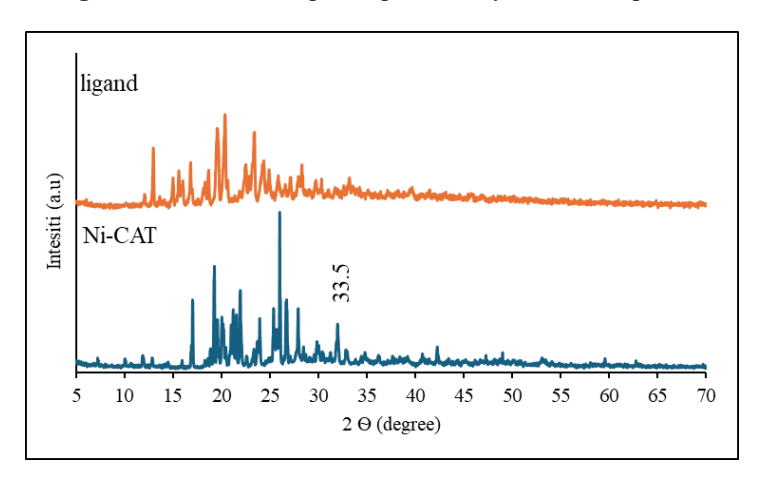


Figure 7. PXRD diffractograms of synthesis compounds

Preliminary complexation study

The UV-Vis titration method was employed to determine the stoichiometric ratio between Ni²⁺

cations and ligands during complex formation. Each titration point, representing the ratio of metal cation to ligand, was plotted as a graph of absorbance

versus [Ni²+]/[L], as shown in **Figure 8**. According to the graph, absorbance increased from 0.085 to 0.086 as the [Ni²+]/[L] ratio rose from 0 to 0.5 [18]. As concentration of the metal ion increased, complexation also increased, until the active binding sites on the ligand became saturated with metal ions. Beyond this point, further increases in metal ion concentration did not significantly affect the absorbance [36].

A noticeable inflection point occurred at a [Ni²⁺]/[L] ratio of 0.5, indicating a 1:2 stoichiometric ratio in the complex formation. This suggested that each Ni²⁺ cation coordinated with two benzimidazole ligands. This finding provided important insights into the composition and structural arrangement of the Ni-CAT coordination complex, emphasising the specific coordination behaviour and interaction between Ni²⁺ and the ligand [37]. Proposed general reaction for the complexation is as follows:

$$Ni^{2+} + 2[L] \longrightarrow 2[L]-Ni$$
 (Eq. 1)

Catalytic activity study

The catalytic performance of Ni-CAT was studied by using various aryl bromides, solvents, and bases. All reactions were carried out by using 0.25 mmol% of catalyst for 2 h under reflux conditions. **Table 5** presents the results obtained from GC-FID analysis.

Tested substrates, aryl bromide with electron-withdrawing groups (EWGs) 1-bromo-4-nitrobenzene in methanol with K₂CO₃ as the base gave the highest conversion rate of 91.66% (entry 1). In contrast, aryl bromides bearing electron-donating groups (EDGs) at the para position, such as -OCH₃, exhibited significantly lower reactivity, with a conversion rate of only 21.20% (entry 4). The electronic properties of substituents influenced the reactivity of the aryl halide in oxidative addition, facilitated transmetalation and reductive elimination steps during catalytic reaction.

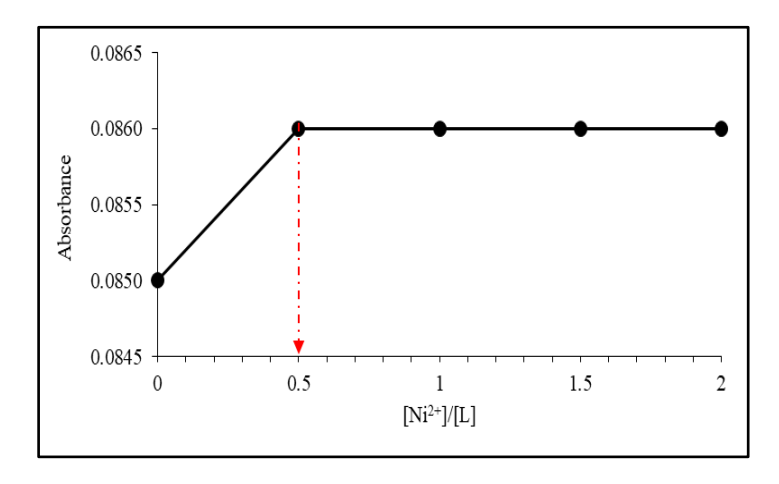


Figure 8. The graph plotted based on absorbance versus [Ni²⁺]/[L]

Table 5. The results of catalytic activity study in Suzuki reaction

Entry	R	Solvent	Base	Conversion Rate (%)	Turnover Number (TON)
1	-NO ₂	MeOH	K ₂ CO ₃	91.66	366.64
2	-H	MeOH	K_2CO_3	37.28	149.12
3	-COCH ₃	MeOH	K_2CO_3	22.13	88.52
4	-OCH ₃	MeOH	K_2CO_3	21.20	84.8
5	$-NO_2$	MeOH	Na_2CO_3	79.06	316.25
6	$-NO_2$	MeOH	NaOAc	69.06	276.25
7	$-NO_2$	MeOH	Et_3N	65.86	263.64
8	$-NO_2$	DMA	K_2CO_3	52.20	208.80
9	$-NO_2$	DMSO	K_2CO_3	46.67	185.88

Oxidative addition Figure 9(a) was the initial and critical step in the catalytic cycle, where the Ni(0) catalyst reacted with the aryl halide, leading to the formation of a Ni(II) aryl complex. The nature of substituents on the aryl halide significantly influenced this step. EWGs, such as -NO2, enhanced the electrophilicity of the aryl halide, facilitating oxidative addition by stabilising the resulting intermediate. This effect was attributed to the resonance and inductive effects that decrease electron density on the aryl ring, making the adjacent carbonbromine bond more electrophilic [38]. In contrast, aryl halides with EDGs, like -OCH3, tend to destabilise the oxidative addition step by reducing the electrophilicity of carbon-bromine bond, which can hinder reactivity and thus led to lower conversion rates [39].

Following by the transmetalation steps Figure 9(b) involves the transfer of the organoboron species (phenylboronic acid) to the nickel intermediate. The efficiency of this step was also greatly affected by the functional groups on aryl halides. For substrates with EWGs, stabilisation of negative charge during this transfer process was enhanced, facilitating bond formation with nickel species. Conversely, the slower transmetalation rate observed with EDGs could be attributed to the electron-rich nature of the intermediates formed in their presence. While stronger basicity in the solvent could enhance transmetalation steps, it was also noted that the polarity of solvent affected the reaction rates, with

more polar solvents stabilizing charged intermediates formed during transmetalation [40].

The final step in the catalytic cycle involved the reductive elimination **Figure 9(c)** of the newly formed C-C bond from the Ni(II) complex, restoring the Ni(0) catalyst. Nature of the departing groups and electronic environment surrounding the nickel centre played a crucial role in determining the efficiency of this step. For EWGs, stabilisation during electron transfer can promote faster reductive elimination, essential for achieving high turnover numbers. In contrast, substrates with EDGs may lead to slower rates of reductive elimination due to unfavourable electronic interactions and steric hindrance [41, 42]. Therefore, the presence of -NO₂ as an EWG resulted in better catalytic performance as compared to -H (entry 2), -COCH₃ (entry 3) and -OCH₃ (entry 4) [10, 32].

The catalytic activity of Ni-CAT was also evaluated under different reaction conditions, including variations in base (entry 1, 5, 6, and 7) and solvent (entry 1, 8, and 9). These tests were conducted by using 1-bromo-4-nitrobenzene and phenylboronic acid. The combination of K₂CO₃ and MeOH resulted in the highest conversion, likely due to the stronger basicity provided by the inorganic base. Additionally, MeOH proved to be a more effective solvent as compared to DMA and DMSO. This was likely due to its ability to dissolve K₂CO₃ more efficiently. As a protic solvent, MeOH could act as a hydrogen bond donor, enhancing the reaction efficiency further [43].

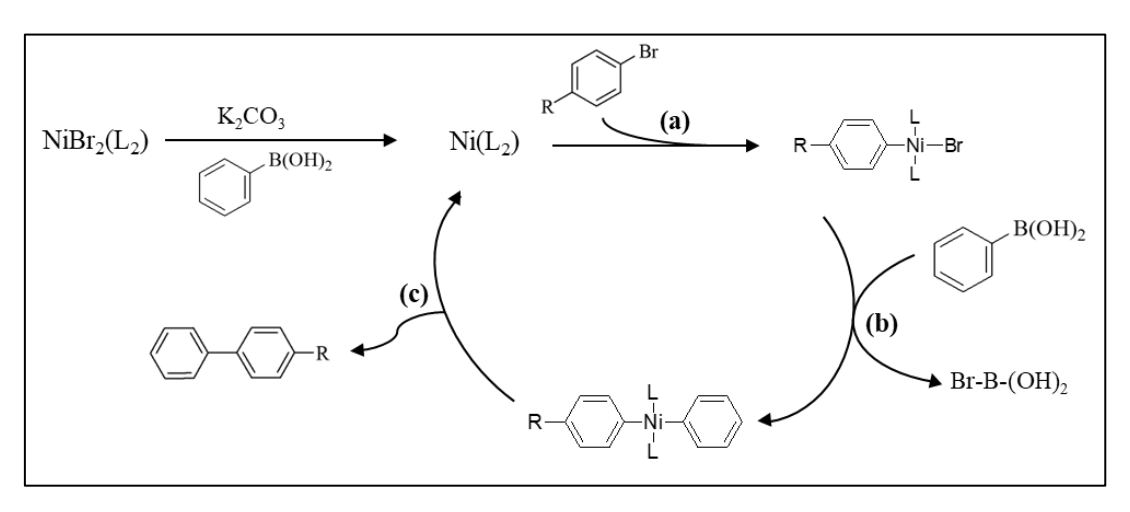


Figure 9. Mechanism of Suzuki reaction by using Ni-CAT as catalyst with differences aryl bromide (R= -NO₂, -H, -OCH₃, and -COCH₃; NiBr₂(L₂) = Ni-CAT)

Conclusion

This study successfully synthesised a benzimidazolebased ligand and its nickel complex (Ni-CAT). The structures of both ligand and complex were confirmed by using FTIR, NMR, UV-Vis spectroscopy, and PXRD analysis. The Ni-CAT complex demonstrated a promising catalytic performance in the Suzuki reaction, achieving a high conversion rate of 91.66% under optimised conditions (0.25 mmol% catalyst loading, MeOH as solvent, and K2CO3 as base) for the carbon-carbon 1-bromo-4-nitrobenzene coupling of with phenylboronic acid.

Despite these encouraging results, this work has certain limitations. The study was restricted to homogeneous catalysis and a narrow substrate scope, and recyclability or long-term stability tests were not conducted, which limited its direct applicability in sustainable or industrial-scale processes. Therefore, future work should explore the immobilisation of Ni-CAT on solid supports to enhance reusability, extend its applicability toward more challenging substrates such as aryl chlorides, and investigate large-scale or continuous-flow reactions.

Acknowledgement

The authors are grateful to the Universiti Teknologi MARA(UiTM), Cawangan Negeri Sembilan, Kampus Kuala Pilah for generously providing the research material, equipment, and instruments.

References

- El-Maiss, J., Mohy El Dine, T., Lu, C. S., Karamé, I., Kanj, A., Polychronopoulou, K., and Shaya, J. (2020). Recent advances in metalcatalyzed alkyl-boron (C(sp³))–C(sp²)) Suzuki-Miyaura cross-couplings. *Catalysts*, 10(3): 296.
- Jarvo, E. R., Wong, C. D., Bradford, L. C., and Hirbawi, N. (2025). Nickel-catalyzed Suzuki-Miyaura cross - coupling reaction of aliphatic alcohol derivatives. *Angewandte Chemie International Edition*, 2025: e202509657.
- Cao, J., Xiong, G., Luo, Z., Huang, Q., Zhou, W., Dragutan, I., Dragutan, V., Sun, Y., and Ding, F. (2024). Synthesis of amide functionlized bidentate NHC-Pd complex for application as catalyst in Suzuki-Miyaura crosscoupling, in distilled water, under mild reaction conditions. *Inorganica Chimica Acta*, 568: 122076.
- Baviskar, B. A., Ajmire, P. V., Chumbhale, D. S., Khan, M. S., Kuchake, V. G., Singupuram, M., and Laddha, P. R. (2023). Recent advances in nickel catalyzed Suzuki-Miyaura cross coupling reaction via CO & CN bond

- activation. Sustainable Chemistry and Pharmacy, 32: 100953.
- John, M. E., Nutt, M. J., Offer, J. E., Duczynski, J. A., Yamazaki, K., Miura, T., Moggach, S. A., Koutsantonis, G. A., Dorta, R., and Stewart, S. G. (2025). Efficient nickel precatalysts for Suzuki-Miyaura cross - coupling of aryl chlorides and arylboronic acids under mild conditions. Angewandte Chemie International Edition, 64(22): e202504108.
- 6. Key, R. J. (2019). Development of nickel catalyzed cross-coupling methodologies. *The Journal of The Royalty Society of Chemistry*, 11: 4287-4296.
- 7. Wu, C., Lin, J., and Tian, X. (2022). Synthesis of indolo [2, 1-a] isoquinolines by nickel-catalyzed Mizoroki–Heck/amination cascade reaction. *Organic letters*, 25(1): 158-162.
- 8. Lin, J., Wu, C., and Tian, X. (2022). Nickel-catalyzed cascade reaction of 2-vinylanilines with gem-dichloroalkenes. *Organic Letters*, 24(27): 4855-4859.
- Zahakifar, F., Keshtkar, A. R., and Talebi, M. (2021).Synthesis of sodium (SA)/polyvinyl alcohol (PVA)/polyethylene (PEO)/ZSM-5 zeolite hybrid oxide nanostructure adsorbent by casting method for uranium (VI) adsorption from aqueous solutions. Progress in Nuclear Energy, 134: 103642.
- Fauzi, A. A., Rahman, N. A. A., and Said, N. R. (2023). Synthesis and characterisations of nickel (II)–hydrazone complex as catalyst in Suzuki reaction. *Malaysian Journal of Analytical Sciences*, 27(3): 453-462.
- Lee, B. C., Liu, C. F., Lin, L. Q. H., Yap, K. Z., Song, N., Ko, C. H. M., Chan, P. H., and Koh, M. J. (2023). N-heterocyclic carbenes as privileged ligands for nickel-catalysed alkene functionalisation. *Chemical Society Reviews*, 52(9): 2946-2991.
- 12. Buldurun, K., and Özdemir, İ. (2019). 5-nitrobenzimidazole containing Pd(II) catalyzed C-C cross- coupling reactions: The effect of the *N*-substituent of the benzimidazole structure on catalyst activity. *Journal of Molecular Structure*, 1192: 172-177.
- 13. Umar, I. K., and Samir, B. (2019). Application of heterocyclic compounds as catalysts in Suzuki-Miyaura cross-coupling reaction. cumhuriyet science. *Journal CSJ.*, 40(4): 854-850
- Yilmaz, Ü., Küçükbay, H., Deniz, S., and Şireci, N. (2013). Synthesis, characterization and microwave- promoted catalytic activity of novel N-phenylbenzimidazolium salts in Heck-Mizoroki and Suzuki- Miyaura cross-coupling

- reactions under mild conditions. *Molecules*, 18(3): 2501-2517.
- Said, N. R., Rezayi, M., Narimani, L., Manan, N. S. A., and Alias, Y. (2015). A novel potentiometric self-plasticizing polypyrrole sensor based on a bidentate bis-NHC ligand for determination of Hg(II) cation. RSC Advances, 5(93): 76263-76274.
- Said, N. R., Rezayi, M., Narimani, L., Al-Mohammed, N. N., Manan, N. S. A., and Alias, Y. (2016). A new N-heterocyclic carbene ionophore in plasticizer-free polypyrrole membrane for determining Ag⁺ in tap water. *Electrochimica Acta*, 197: 10-22.
- 17. Horak, E., Vianello, R., and Steinberg, I. M. (2019). Chemistry and applications of benzimidazole and its derivatives. *Optical sensing (nano) materials based on benzimidazole derivatives*. IntechOpen, pp. 159.
- Said, N. R., Mustakim, M. A., Sani, N. M., and Baharin, S. N. A. (2018). Heck reaction using palladium-benzimidazole catalyst: Synthesis, characterisation and catalytic activity. In *IOP Conference Series: Materials Science and Engineering*, 458(1), 012019.
- 19. Wang, T., Wei, T. R., Huang, S. J., Lai, Y. T., Lee, D. S., and Lu, T. J. (2021). Synthesis of xylyl-linked bis-benzimidazolium salts and their application in the palladium-catalyzed Suzuki–Miyaura cross-coupling reaction of aryl chlorides. *Catalysts*, 11(7): 817.
- 20. Nair, P. P., Jayaraj, A., and Swamy P, C. A. (2022). Recent advances in benzimidazole based NHC-metal complex catalysed cross-coupling reactions. *ChemistrySelect*, 7(4): e202103517.
- 21. Gholivand, K., Salami, R., Farshadfar, K., and Butcher, R. J. (2016). Synthesis and structural characterization of Pd(II) and Cu(I) complexes containing dithiophosphorus ligand and their catalytic activities for Heck reaction. *Polyhedron*, 119: 267-276.
- Kucukbay, H., Yilmaz, Ü., Yavuz, K., and Bugday, N. (2015). Synthesis, characterization, and microwave- assisted catalytic activity in Heck, Suzuki, Sonogashira, and Buchwald-Hartwig cross-coupling reactions of novel benzimidazole salts bearing N-phthalimidoethyl and benzyl moieties. *Turkish Journal of Chemistry*, 39(6): 1265-1278.
- 23. Ado, I., Na'aliya, J., Sani, S., and Haleelu, M. M. (2021). Synthesis, spectroscopic and antimicrobial studies of Co(II), Ni(II), Cu(II) and Zn(II) complexes derived from benzoic acid bidentate Schiff base ligand. *Journal of Applied Sciences and Environmental Management*, 25(9): 1599-1603.

- 24. Haque, R. A., and Iqbal, M. A. (2013). Synthesis and characterization of ortho-xylyl linked bis- benzimidazolium salts (Part-II). *Asian Journal of Chemistry*, 25(6): 3049.
- Thanneeru, S., Ayers, K. M., Anuganti, M., Zhang, L., Kumar, C. V., Ung, G., and He, J. (2020). N-Heterocyclic carbene-ended polymers as surface ligands of plasmonic metal nanoparticles. *Journal of Materials Chemistry C*, 8(7): 2280-2288.
- Rahman, M. M., Zhao, Q., Meng, G., Szostak, R., and Szostak, M. (2022). [Ni (Np#)(η5-Cp) Cl]: Flexible, Sterically Bulky, Well-Defined, Highly Reactive Complex for Nickel-Catalyzed Cross-Coupling. *Organometallics*, 41(18):2597-2604.
- 27. Kulaksizoğlu, S., Gökçe, C., and Gup, R. (2012). Asymmetric BIS (bidentate) azine ligand and transition metal complexes: Synthesis, characterization, DNA-binding and cleavage studies and extraction properties for selected metals and dichromate anions. *Journal of the Chilean Chemical Society*, 57(3): 1213-1218.
- 28. Hao, Z. C., Wang, S. C., Yang, Y. J., and Cui, G. H. (2020). Syntheses, structural diversities and photocatalytic properties of three nickel (II) coordination polymers based semi-bis (benzimidazole) and aromatic dicarboxylic acid ligands. *Polyhedron*, 181: 114466.
- Hou, C. L., Song, J. X., Chang, X., and Chen, Y. (2024). Photoluminescent nickel (II) carbene complexes with ligand-to-ligand charge-transfer excited states. *Chinese Chemical Letters*, 35(1): 108333.
- Dong, X. Y., Kang, Q. P., Jin, B. X., and Dong, W. K. (2017). A dinuclear nickel (II) complex derived from an asymmetric Salamo-type N₂O₂ chelate ligand: Synthesis, structure and optical properties. *Zeitschrift für Naturforschung B*, 72(6): 415-420.
- Ting, S. I., Garakyaraghi, S., Taliaferro, C. M., Shields, B. J., Scholes, G. D., Castellano, F. N., and Doyle, A. G. (2020). 3d-d excited states of Ni (II) complexes relevant to photoredox catalysis: spectroscopic identification and mechanistic implications. *Journal of the American Chemical Society*, 142(12): 5800-5810.
- 32. Golestanzadeh, M., and Naeimi, H. (2019). Palladium decorated on a new dendritic complex with nitrogen ligation grafted to graphene oxide: Fabrication, characterization, and catalytic application. *RSC Advances*, *9*(47): 27560-27573.
- 33. Jaji, N. D., Othman, M. B. H., Lee, H. L., Hussin, M. H., and Hui, D. (2021). One-pot

- solvothermal synthesis and characterization of highly stable nickel nanoparticles. *Nanotechnology Reviews*, 10(1): 318-329.
- 34. Tang, S., Li, L., Cao, X., and Yang, Q. (2023). Ni-chitosan/carbon nanotube: An efficient biopolymer-inorganic catalyst for selective hydrogenation of acetylene. *Heliyon*, 9(2): e13523.
- 35. Moreira, J. M., Vieira, S. D. S. F., Correia, G. D. D., de Almeida, L. N., Finoto, S., Brandl, C. A., Msumange, A.A., Galvão, F., Pires de Oliveira, K.M., Caneppele Paveglio, G., da Silva, M.M., Tirloni, B., de Carvalho, C. T., and Roman, D. (2025).Synthesis of Characterization Novel Hydrazone Complexes: Exploring DNA/BSA Binding and Antimicrobial Potential. ACS Omega, 10(7): 7428-7440.
- 36. Mrudula, M. S., and Gopinathan Nair, M. R. P. (2020). Studies on the complexation of 3D transition metal ions with NR/PEO block copolymer in aqueous medium. *Polymer Engineering & Science*, 60(4): 661-672.
- 37. Abd El-Lateef, H. M., Khalaf, M. M., and Abdou, A. (2024). Exploring the molecular structure and in vitro biological potential of newly synthesized Fe (III), Co (II), and Ni (II) coordination compounds with 2-(pyridin-2-yl)-1H-benzimidazole and phenylalanine ligands. *Polyhedron*, 260: 117103.
- 38. Luo, J., Davenport, M. T., Ess, D. H., and Liu, T. L. (2024). Nickel catalyzed electrochemical

- cross electrophile C(sp²)–C(sp³) coupling via a Ni(II) aryl amido intermediate. *Angewandte Chemie*, 136(38): e202407118.
- Luo, J., Davenport, M. T., Callister, C., Minteer, S. D., Ess, D. H., and Liu, T. L. (2023). Understanding formation and roles of Ni(II) aryl amido and NiIII aryl amido intermediates in Ni-catalyzed electrochemical aryl amination reactions. *Journal of the American Chemical Society*, 145(29): 16130-16141.
- 40. Buchspies, J., Rahman, M. M., and Szostak, M. (2020). Suzuki–Miyaura cross-coupling of amides using well-defined, air-and moisture-stable nickel/NHC (NHC=N-Heterocyclic Carbene) complexes. *Catalysts*, 10(4): 372.
- Lau, S. H., Borden, M. A., Steiman, T. J., Wang, L. S., Parasram, M., and Doyle, A. G. (2021). Ni/photoredox-catalyzed enantioselective crosselectrophile coupling of styrene oxides with aryl iodides. *Journal of the American Chemical Society*, 143(38): 15873-15881.
- 42. Zhang, T., Zhong, K., Lin, Z. K., Niu, L., Li, Z. Q., Bai, R., Engle, K. M., and Lan, Y. (2023). Revised Mechanism of C(sp³)–C(sp³) reductive elimination from Ni (II) with the assistance of a z-type metalloligand. *Journal of the American Chemical Society*, 145(4): 2207-2218.
- 43. Elhage, A., Lanterna, A. E., and Scaiano, J. C. (2018). Light-induced sonogashira C–C coupling under mild conditions using supported palladium nanoparticles. *ACS Sustainable Chemistry & Engineering*, 6(2): 1717-1722.